How Does Stochastic Ryanodine Receptor-Mediated Ca Leak Fail to Initiate a Ca Spark?

Daisuke Sato and Donald M. Bers*
Department of Pharmacology, University of California, Davis, California

ABSTRACT Spontaneous calcium (Ca) sparks are initiated by single ryanodine receptor (RyR) opening. Once one RyR channel opens, it elevates local [Ca] in the cleft space ($[Ca]_{Cleft}$), which opens other RyR channels in the same Ca release unit (CaRU) via Ca-induced Ca-release. Experiments by Zima et al. (*J. Physiol.* 588:4743–4757, 2010) demonstrate that spontaneous Ca sparks occur only when intrasarcoplasmic-reticulum (SR) [Ca] ($[Ca]_{SR}$) is above a threshold level, but that RyR-mediated SR Ca leak exists without Ca sparks well below this threshold $[Ca]_{SR}$. We examine here how single RyR opening at lower $[Ca]_{SR}$ can fail to recruit Ca sparks at a CaRU, while still contributing to SR Ca leak. We assess this using a physiologically detailed mathematical model of junctional SR Ca release in which RyR gating is regulated by $[Ca]_{SR}$ and $[Ca]_{Cleft}$. We find that several factors contribute to the failure of Ca sparks as $[Ca]_{SR}$ declines: 1), lower $[Ca]_{SR}$ reduces driving force and thus limits local $[Ca]_{Cleft}$ achieved and the rate of rise during RyR opening; 2), low $[Ca]_{SR}$ limits RyR open time (τ_O), which further reduces local $[Ca]_{Cleft}$ attained; 3), low τ_O and fast $[Ca]_{Cleft}$ dissipation after RyR closure shorten the opportunity for neighboring RyR activation; 4), at low $[Ca]_{SR}$, the RyR exhibits reduced $[Ca]_{Cleft}$ sensitivity. We conclude that all of these factors conspire to reduce the probability of Ca sparks as $[Ca]_{SR}$ declines, despite continued RyR-mediated Ca leak. In addition, these same factors explain the much lower efficacy of L-type Ca channel opening to trigger local SR Ca release at low $[Ca]_{SR}$ during excitation-contraction coupling. Conversely, all of these factors are fundamentally important for increasing the propensity for pro-arrhythmic Ca sparks and waves in cardiac myocytes at high $[Ca]_{SR}$.

INTRODUCTION

Calcium (Ca) sparks and Ca leak from the sarcoplasmic reticulum (SR) play an important role in excitation-contraction coupling (ECC) (1–3). Recent experimental results have shown that there is ryanodine-receptor (RyR)-mediated SR Ca leak that is not evident as Ca sparks (4,5). Zima et al. (5) measured SR Ca leak directly as the rate of decline of intra-SR [Ca] ($[Ca]_{SR}$) upon complete block of the SR Ca-ATPase. They found that Ca-spark frequency declines as $[Ca]_{SR}$ declines, but that sparks abruptly disappear at an apparent $[Ca]_{SR}$ threshold, despite continued RyR-mediated leak at very low $[Ca]_{SR}$. According to these and other results, as $[Ca]_{SR}$ increases to high levels, spontaneous Ca sparks occur more frequently. On the other hand, when $[Ca]_{SR}$ is at moderate to low levels, Ca leak via RyRs still occurs, but Ca sparks are not observed.

In cardiac myocytes, most RyRs are located in clusters in the SR where the SR comes near the plasma membrane, forming a small cleft space continuous with the cytosol and submembrane space. Each cluster contains several to several hundred RyRs (6–8) and is called a Ca-release unit (CaRU). RyR channel gating is sensitive to the cleft-space [Ca] ($[Ca]_{Cleft}$) and to $[Ca]_{SR}$ (1,9–12). Before a Ca-spark or Ca-leak event, the RyRs in a CaRU are all in a closed state. During ECC, $[Ca]_{Cleft}$ rises due to Ca influx via L-type Ca channels or Ca diffusion from neighboring CaRUs, activating RyR channel opening to release more Ca from the SR (Ca-induced Ca-release (13,14)). Even without L-type Ca-channel opening RyR channels open stochastically at rates depending on $[Ca]_{Cleft}$ and $[Ca]_{SR}$ (and also regulatory factors such as redox state and phosphorylation (1–3)). Once one RyR channel opens stochastically and elevates $[Ca]_{Cleft}$ locally, it is expected to recruit neighboring RyRs in the CaRU to open, resulting in a Ca spark where 6–20 RyRs open to produce the local Ca flux (1,15). Because of the large Ca current through a single RyR under physiological conditions (0.35–0.6 pA at 1 mM $[Ca]_{SR}$) (16,17), one would expect local $[Ca]_{Cleft}$ to rapidly rise to >10 μM (1,18) and effectively trigger opening of other RyRs in the CaRU and thus a Ca spark. The findings that substantial SR Ca leak via RyRs occurs without producing Ca sparks (4,5) raise the question that is the focus of this report: how does RyR opening at a CaRU fail to trigger a Ca spark at moderate to low $[Ca]_{SR}$?

The probability of RyR transition from the closed to open state depends on several factors that are examined here. Reducing $[Ca]_{SR}$ will lower the RyR driving force, thereby limiting peak $[Ca]_{Cleft}$ at all times after opening. If openings are briefer at low $[Ca]_{SR}$ (as measured experimentally (19)), $[Ca]_{Cleft}$ may be reduced and the duration of $[Ca]_{Cleft}$ elevation will be shorter. It should be noted that $[Ca]_{Cleft}$ is expected to drop toward diastolic levels very rapidly once the RyR closes (<2 ms) (1,18). Thus, if no new RyR opening occurs stochastically during this open time and $[Ca]_{Cleft}$ decline, then a potential spark will be aborted, and $[Ca]_{Cleft}$ will fall back to the resting level (sometimes referred to as stochastic attrition (20,21)). Lower $[Ca]_{SR}$ also reduces the

Submitted June 7, 2011, and accepted for publication October 12, 2011.

*Correspondence: dmbers@ucdavis.edu

Editor: David A. Eisner.

0006-3495/11/11/2370/10 $2.00

doi: 10.1016/j.bpj.2011.10.017

sensitivity of RyR to $[Ca]_{Cleft}$ (9), which may reduce the probability that a single RyR opening will trigger neighboring RyRs within a CaRU. Here, we quantitatively analyze all of these factors that may contribute to Ca-spark failure with continued RyR-mediated leak in ventricular myocytes. Fig. 1 *A* demonstrates visually the CaRU working hypothesis that at relatively high $[Ca]_{SR}$, one RyR opening suffices to robustly initiate a Ca spark (Fig. 1 *A*, *lower left*) where multiple RyRs open in concert (Fig. 1 *A*, *middle* and *right*).

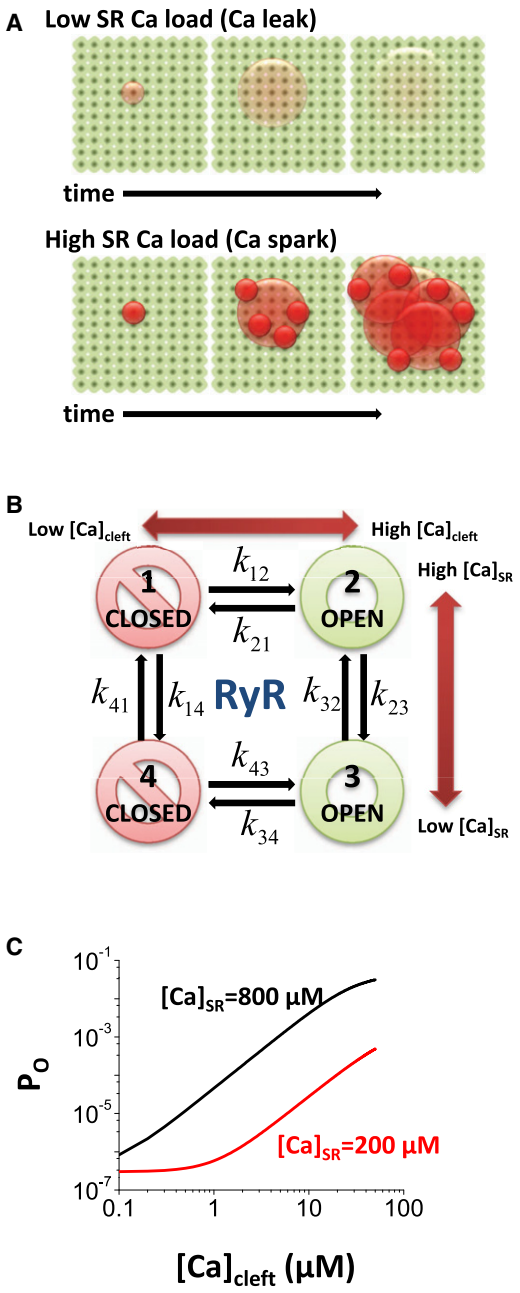

FIGURE 1 (*A*) Schematic illustration of CaRU RyR array (*green spheres*), Ca leak (*upper*), and a Ca spark (*lower*). (*B*) RyR gating scheme. (*C*) Open probability (P_o) of RyR as a function of $[Ca]_{Cleft}$ for two levels of $[Ca]_{SR}$.

In contrast, at low $[Ca]_{SR}$ (Fig. 1 *A*, *upper*) single RyR openings may be less able to recruit neighboring RyRs, and the potential spark fails.

MATERIALS AND METHODS

To understand the mechanisms of the Ca spark and Ca leak, we use a physiologically detailed subcellular Ca cycling model based on that developed by Restrepo et al. (22). Details of the model are in the Supporting Material. Here, we highlight several key points.

The RyR channel is modeled as a four-state Markovian model regulated by $[Ca]_{Cleft}$ and $[Ca]_{SR}$ (Fig. 1 *B*). The ~30-pL model myocyte contains 19,305 CaRUs, and a single CaRU contains 100 RyRs (Fig. 1 *A*). Each RyR opens independently and stochastically. The average volume of the cleft space is 0.00126 μm^3 (disk of radius 0.2 μm and depth 10 nm). Several changes were made to the Restrepo et al. model, including

1. The rates from the closed state to the open state,

$$k_{12} = \frac{K_u c_p^2}{K_{cp}^2 + c_p^2} + w, \quad k_{43} = \frac{K_b c_p^2}{K_{cp}^2 + c_p^2} + w,$$

where k_{12} is the rate from state 1 (S1) in Fig. 1 *B* to S2; k_{43} is the rate from S4 to S3; c_p is $[Ca]_{Cleft}$; and K_u, K_{cp}, K_b, and w are constants. This change limits the number of RyR openings during a Ca spark to ~10. For our conditions, unitary RyR current is 0.51 pA at $[Ca]_{SR} - [Ca]_{Cleft} = 1$ mM.

2. The rates from the open state to the closed state, to fit the experimental observation of the mean open times (0.7~1.9 ms) (19):

$$k_{21} = 0.5 \text{ ms}^{-1}, \quad k_{34} = 3.3 \text{ ms}^{-1}.$$

A detailed discussion of equations and parameters can be found in the Supporting Material, including Table S1, which specifies changes made to the published Restrepo model. In this study, we focus on RyR gating that is independent of L-type Ca-channel gating, so L-type Ca current was set to zero except in ECC simulations. We also added background sarcolemmal membrane Ca flux (I_{CaBk}) and the sarcolemmal membrane Ca pump (I_{SLCaP}) from the Shannon-Bers model (23). Membrane voltage (V_m) was fixed (−80 mV) except during ECC simulations. To avoid initial condition dependence for the results, all simulations were evaluated after steady state was reached.

Ca sparks and nonspark Ca leak via RyRs (referred to as non-spark leak) are determined based on the amplitude of the local elevation of cytosolic [Ca] within a volume of 0.5 μm^3 surrounding a given CaRU. In experiments, nonspark-mediated Ca leak is not readily detectable because of noise in the $[Ca]_i$ signal. In computer simulations, of course, we can detect any Ca leak. To mimic the experimental detection threshold for Ca sparks, we set 0.1 μM for the $\Delta[Ca]_i$ threshold amplitude for Ca sparks (i.e., if the amplitude is <0.1 μM, we call it nonspark leak). This is close to the minimum Ca-spark amplitude detected by Picht et al. in their spark analysis algorithm (~0.06 μM), which is also sensitive to experimental conditions (24). Fig. S2 shows a histogram of a Ca-release event amplitude from our simulation, illustrating the cut-off amplitude used for Ca sparks. Fig. S3 shows three sample events from our simulations, where we added artificial Gaussian noise to mimic experimental noise (the upper two events in Fig. S3 qualified as Ca sparks). As the detection threshold increases, nonspark leak is increased (25). If we reduce our detection threshold to $\Delta[Ca]_I = 0.05$ μM, more Ca sparks are seen (Fig. S4), but our conclusions are unaltered.

To examine the efficacy of L-type Ca current during ECC, we use the original Restrepo model for L-type Ca current. V_m is held at −80 mV for 2 s, and a square voltage-clamp pulse is then applied for 200 ms. Gain is calculated as the integral of the SR release current divided by the integral of the Ca current.

RESULTS

Influence of $[Ca]_{SR}$ and $[Ca]_{Cleft}$ on probability of RyR opening

The RyR is regulated by both $[Ca]_{Cleft}$ and $[Ca]_{SR}$. If $[Ca]_{Cleft}$ is elevated, the probability of opening becomes higher. This probability also depends on $[Ca]_{SR}$ (19), and this joint dependence on $[Ca]_{SR}$ and $[Ca]_{Cleft}$ is shown in Fig. 1, *B* and *C*.

We estimate $[Ca]_{Cleft}$ when a single RyR channel opens in the CaRU. In other words, if one RyR channel opens, how quickly does $[Ca]_{Cleft}$ rise to steady state (where Ca diffusion into and out of the cleft are equal)? The driving force of SR Ca release ($[Ca]_{SR} - [Ca]_{Cleft}$) depends mainly on $[Ca]_{SR}$ and less on $[Ca]_{Cleft}$, because $[Ca]_{SR}$ (~1 mM) is much higher than $[Ca]_{Cleft}$. Due to driving force, as $[Ca]_{SR}$ increases, $[Ca]_{Cleft}$ accumulates faster and to a higher level (Fig. 2 *A*). For the $[Ca]_{SR}$ of 200 and 800 μM shown, there is a roughly fourfold difference in driving force. The secondary rise in $[Ca]_{Cleft}$ at >2 ms reflects the gradual rise in submembrane [Ca], which slows Ca diffusion out of the cleft.

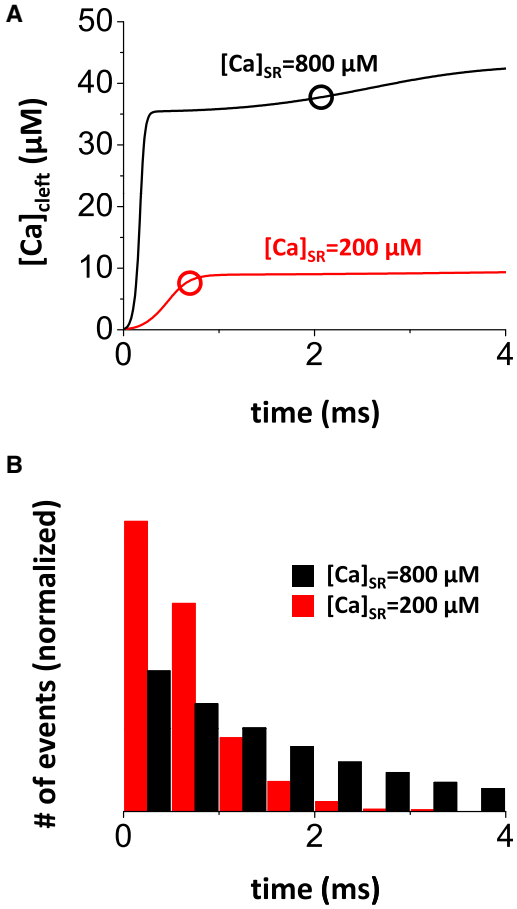

FIGURE 2 (*A*) Ca accumulation in the cleft space during single RyR opening with low ($[Ca]_{SR}$ = 200 μM) and high ($[Ca]_{SR}$ = 800 μM) SR Ca load. Circles indicate mean open time for each case. Slow increase of $[Ca]_{Cleft}$ at 1–4 ms reflects slow accumulation of [Ca] at the submembrane space. (*B*) Normalized open-time distribution for simulated events.

The mean open time of the RyR is also influenced by $[Ca]_{SR}$ (19). In our model, the mean open times (τ_O) at 200 and 800 μM $[Ca]_{SR}$ are ~0.7 and 2 ms, respectively. The distribution of open time is exponential, and the number of events declines with increasing τ_O. It should be noted that opening events with open time shorter than the mean occur with much higher frequency (Fig. 2 *B*). Thus, a large fraction of openings are shorter in duration at the lower values of $[Ca]_{SR}$.

The increased driving force and prolonged open time contribute to higher and longer-lasting $[Ca]_{Cleft}$ during a single RyR opening at 800 mM $[Ca]_{SR}$, reaching ~37 μM within the mean open time (Fig. 2 *A*, *black circle*) versus ~8 μM at $[Ca]_{SR}$ = 200 μM (Fig. 2 *A*, *red circle*).

Next, we estimate the probability (p) that a single closed RyR channel will open during the time (Δt) after the first RyR opening by

$$p = S_1(1 - \exp(-k_{12}\Delta t)) + S_4(1 - \exp(-k_{34}\Delta t)),$$

where S_n is the fraction of RyR in state n in the four-state Markovian model (Fig. 1 *B*), k_{12} and k_{43} are transition rates from S1 (closed state with low $[Ca]_{Cleft}$/high $[Ca]_{SR}$) to S2 (open state with higher $[Ca]_{Cleft}$) and S4 (closed state with low $[Ca]_{Cleft}$ and $[Ca]_{SR}$) to S3 (open state with high $[Ca]_{Cleft}$), respectively. Circles in Fig. 3 *A* are typical $[Ca]_{Cleft}$ based on the analysis in Fig. 2. The timescale of Δt spans the relevant mean open times. Since the mean open time is longer as $[Ca]_{SR}$ becomes higher, we chose 1–4 ms for high $[Ca]_{SR}$ and 0.5–2 ms for low $[Ca]_{SR}$. Since opening rates (k_{12} and k_{43}) are functions of $[Ca]_{Cleft}$, as $[Ca]_{Cleft}$ is increased, the probability of opening a second RyR increases as $[Ca]_{Cleft}$ increases. The ratio between S1 and S4 depends on $[Ca]_{SR}$. As $[Ca]_{SR}$ rises, the RyR tends to move from S4 to S1 (where it is more readily activated by $[Ca]_{Cleft}$; $k_{12} > k_{43}$). As a result, the curve shifts from red to black in Fig. 3 *A*. Since there are 100 RyRs in one CaRU, if the probability is >5%, several RyRs will open, further increasing $[Ca]_{Cleft}$, and this positive feedback leads to a Ca spark. On the other hand, if the probability is <<1%, then it is most probable that no additional RyRs in the CaRU will open, and the flux from the single RyR opening becomes nonspark Ca leak. In Fig. 3 *A*, Ca sparks and nonspark leak are indicated with gradation from yellow (Ca spark) to green (Ca leak). Because this is a stochastic system, there is no sharp transient between the Ca spark and Ca leak. It should be noted that there is an ~3% probability of triggering a second RyR for 800 μM $[Ca]_{SR}$, whereas this probability is only 0.004% for in the case of 200 μM $[Ca]_{SR}$ (Fig. 3 *A*, *black* and *red circles*, respectively).

To be more precise, the probability ($P(n)$) that n channels open in one CaRU due to single RyR channel opening can be calculated for high $[Ca]_{SR}$ (Fig. 3 *B*) and low $[Ca]_{SR}$ (Fig. 3 *C*) by

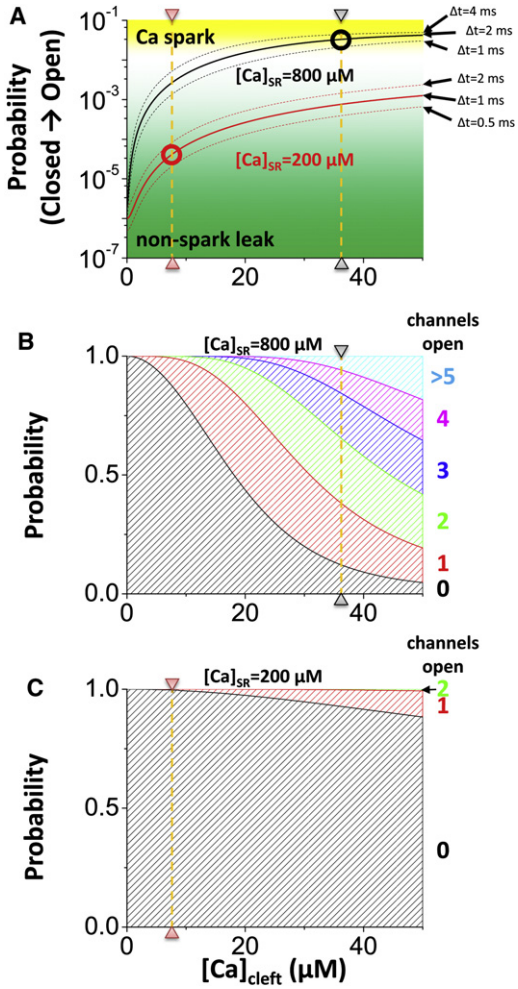

FIGURE 3 (*A*) Probability of transition from the closed to the open state when RyR channel is exposed to $[Ca]_{Cleft}$ for the indicated Δt ms. Circles indicate $[Ca]_{Cleft}$ level if RyR opens for mean open time for each case (*black*, low SR Ca load;, *red*, high SR Ca load). (*B*) Probability that *n* RyR channels will open when the CaRU is exposed to $[Ca]_{Cleft}$ for 2 ms with a high SR Ca load (800 μM). The orange line indicates the $[Ca]_{Cleft}$ level if RyR opens for the mean open time. (*C*) Probability that *n* RyR channels open when the CaRU is exposed to $[Ca]_{Cleft}$ for 1 ms with low SR Ca load (200 μM). The orange line indicates $[Ca]_{Cleft}$ level if RyR opens for the mean open time.

$$P(n) = \begin{bmatrix} N-1 \\ n \end{bmatrix} p^n (1-p)^{N-1-n},$$

where N is the number of RyRs in one CaRU (100 in our model). This is simply a binomial distribution. Since we are calculating whether one RyR opening can open the other RyRs, one RyR channel is already open. Therefore, this one is subtracted from N.

At high $[Ca]_{SR}$, once $[Ca]_{Cleft}$ exceeds 20 μM >50% of the first stochastic RyR openings will open another RyR in the same CaRU (note that typical $[Ca]_{Cleft}$ is 37 μM (Fig. 3 *B*)). On the other hand, at low $[Ca]_{SR}$, stochastic opening of one RyR will not open another RyR in the same CaRU, even if $[Ca]_{Cleft}$ goes to a high regime (<10% at $[Ca]_{Cleft} = 50$ μM, and typical $[Ca]_{Cleft}$ is 8 μM (Fig. 3 *C*)). Note that the multiple channel openings indicated in Fig. 3 *B* are only those opened because of the initial RyR opening and prevailing $[Ca]_{SR}$ and $[Ca]_{cleft}$. Of course, once any additional opening occurs the events will synergize, and a full-blown Ca spark is much more likely to occur. We cover that situation later in our discussion of the full-blown simulations.

Analyses done above are summarized in Fig. 4 as a function of $[Ca]_{SR}$. First, mean open time is an increasing function of $[Ca]_{SR}$ (Fig. 4 *A*). Then, $[Ca]_{Cleft}$ is determined by RyR open time and driving force (Fig. 4 *B*). Since $[Ca]_{Cleft}$ is nearly at steady state within the mean open time, the driving force is the main determinant of the $[Ca]_{Cleft}$. The

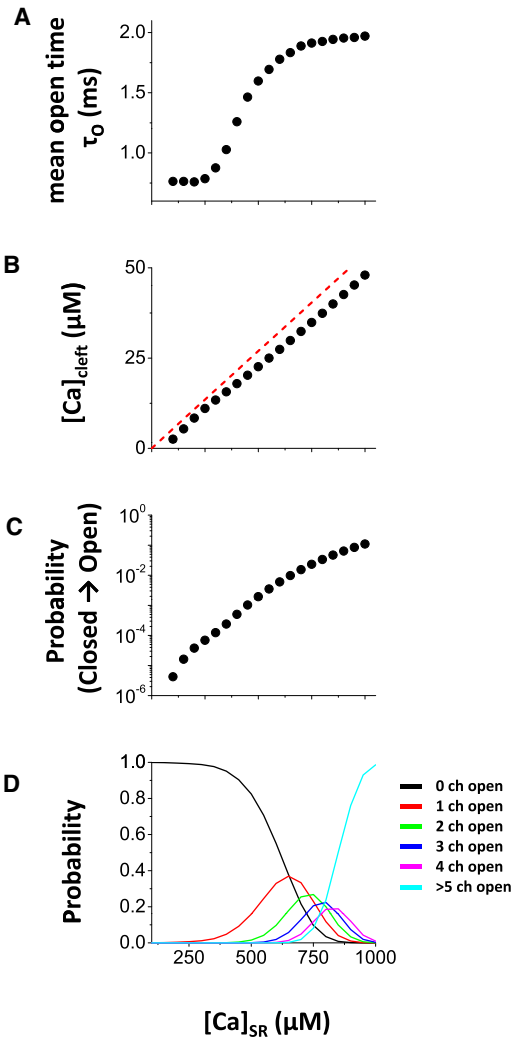

FIGURE 4 $[Ca]_{SR}$ dependence of RyR gating. (*A*) Mean open time versus $[Ca]_{SR}$. (*B*) $[Ca]_{Cleft}$ versus $[Ca]_{SR}$ when a single RyR opens for the mean open time. (*C*) Probability of transition from the closed to the open state when the RyR channel is exposed to $[Ca]_{Cleft}$ for the mean open time. (*D*) Probabilities that n RyR channels open when the CaRU is exposed to $[Ca]_{Cleft}$ for the mean open time.

dashed red line indicates the steady-state $[Ca]_{Cleft}$ for long openings. Then, the probability (p) that a closed RyR channel will open during the mean open time of a first event depends on $[Ca]_{Cleft}$ and the sensitivity of RyR to $[Ca]_{Cleft}$ determined by $[Ca]_{SR}$ (Fig. 4 *C*). As $[Ca]_{SR}$ increases, since p is increased, the number of open RyR channels is increased (Fig. 4 *D*). Note that the probability of three RyR channels opening is vanishingly small for $[Ca]_{SR} \leq 500\ \mu M$, and this could be near the minimum number of RyR openings at a CaRU to trigger a detectable Ca spark. On the other hand, for $[Ca]_{SR} > 750\ \mu M$, Ca sparks are robustly recruited (more than five open channels). Once several RyRs are open, they bring more Ca and open more RyRs. This process is positive feedback for $[Ca]_{SR} = 800\ \mu M$ and is similar to other excitable systems. Fig. S6 shows how a single RyR opening tends toward positive feedback at higher $[Ca]_{SR}$, but tends to extinguish release at lower $[Ca]_{SR}$.

Integrated model of Ca sparks and nonspark-mediated leak

The above analyses imply that the probability of a single RyR opening becoming a Ca spark would rise quickly as SR Ca load becomes higher. However, the synergy is not fully captured by those static snapshots of gating probability. So, we run the full physiological simulation here to assess the recruitment of both Ca sparks and nonspark leak events (Figs. 5 and 6). Initially in Fig. 5 *A*, both Ca sparks and Ca leak occur, but $[Ca]_{SR}$ is at steady state (Fig. 5A). At this steady-state condition for the full model, the SR Ca leak is balanced by reuptake by the SERCA pump (I_{up}), and therefore, $[Ca]_{SR}$ stays constant. Then, steady state is perturbed by blocking the SERCA pump (I_{up}) to simulate the thapsigargin experiments in Fig. 1 *C* of Zima et al. (5). As expected from the above, Ca-spark frequency decreases as $[Ca]_{SR}$ declines (Fig. 5 *A*). Furthermore, Ca sparks are observed until $[Ca]_{SR}$ falls to ~550 μM. Even when $[Ca]_{SR}$ is below this point, $[Ca]_{SR}$ still declines. This means that only nonspark Ca leak exists at lower SR Ca load. In Fig. 5 *B*, a typical CaRU activity from this simulation is shown. As $[Ca]_{SR}$ decreases, the number of open channels during stochastic Ca-release events is decreased (usually to one channel opening, but occasionally to two).

Ca flux rates of Ca sparks and nonspark Ca leak are a function of SR Ca load (Fig. 6 *A*). Since both frequency and driving force are increased as $[Ca]_{SR}$ is increased, the Ca-spark flux steeply increases as a function of $[Ca]_{SR}$. The three curves shown are in reasonable quantitative agreement with experimental measurements in Fig. 6 *A* of Zima et al. (5). Note that in the study presented here, we only consider RyR-mediated leak, whereas there is an additional small RyR-independent leak present in the experimental data (5). If we make a two- to threefold change in RyR

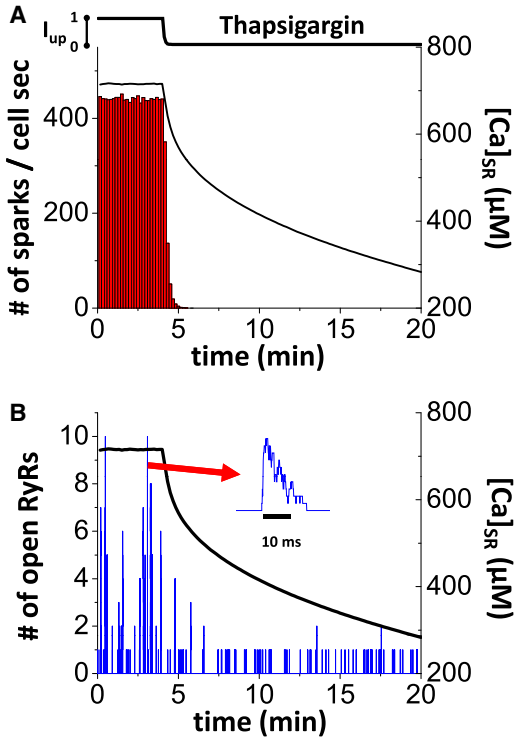

FIGURE 5 Numerical experiment using the physiologically detailed model of Ca cycling. (*A*) Ca-spark frequency and SR Ca load. The SERCA pump (I_{up}) is decreased to simulate thapsigargin exposure. Ca spark frequency (*bars*) and SR Ca load (*line*) versus time. (*B*) Example of single CaRU activity from simulation in *A*. Number of open channels versus time. (*Inset*) A typical Ca spark.

sensitivity to Ca (Ku) or in single-channel flux (J_{max}) individually, these curves are shifted, altering the Ca-spark threshold (Fig. S1), but the qualitative pattern is not appreciably altered.

Altered SR Ca leak-load relationship in heart failure and adrenergic activation

We also tested how these curves shift when RyR channel properties are altered (analogous to either genetic mutations associated with catecholaminergic polymorphic ventricular tachycardia (CPVT) or RyR gating alterations caused by phosphorylation, redox modification, or heart failure (HF)). Here, we chose two cases, HF (Fig. 6 *B*) and isoproterenol (ISO) stimulation (Fig. 6 *C*), using parameter changes based on the work of Shannon et al. (26). Of note here, for HF, SERCA2 uptake V_{max} was reduced by 40%, Na/Ca exchange V_{max} was increased twofold, and SR Ca leak was increased threefold (with a threefold enhancement of Ca affinity). These changes shift all of the leak curves to the left. The Ca-spark curve is especially depressed, and less left-shifted, whereas the nonspark leak is much steeper. This is consistent with the much higher leak rates measured in our rabbit HF model at a given SR Ca load (27), despite

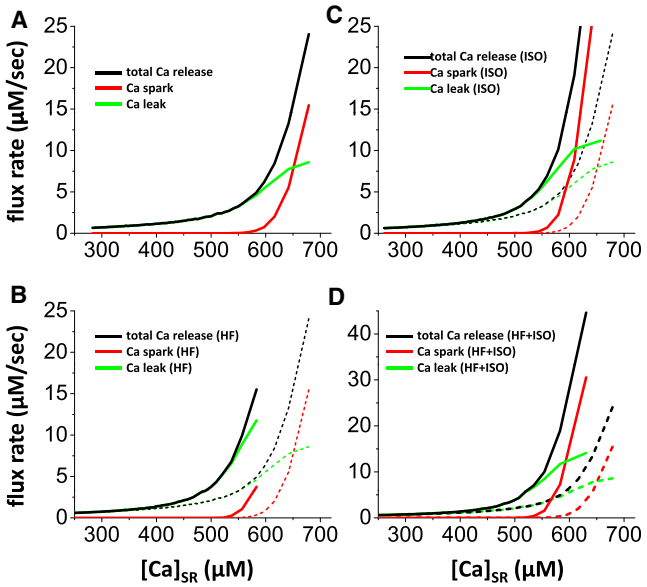

FIGURE 6 SR Ca leak-load relationships. (*A*) Control SR Ca flux rates for total, Ca spark and nonspark Ca leak versus SR Ca load ($[Ca]_{SR}$). (*B*) Same analysis for model adjusted for HF. (*C*) Same analysis for model with ISO adjustments. (*D*) Same analysis when HF is exposed to ISO. Broken curves in *B–D* are data from *A* for comparison.

very low Ca-spark frequencies (D. M. Bers, unpublished observation). With ISO (twofold increase in SERCA2 Ca affinity, 50% decrease in myofilament Ca affinity, and twofold increase in RyR Ca affinity), all three curves were again left-shifted. However, with ISO, as compared to HF, the nonspark leak curve was less shifted and the Ca-spark curve was more shifted, consistent with higher Ca-spark frequency and leak typically seen with ISO (see, e.g., our previous works (28,29). When combining HF and ISO, there is a further increase in the Ca-spark curve, and this would be consistent with an increased propensity for triggered arrhythmias associated with Ca waves in HF (30).

Impact of $[Ca]_{SR}$ on efficacy of Ca-induced Ca-release during ECC

The ability of a given L-type Ca current to trigger SR Ca release also depends steeply upon $[Ca]_{SR}$, and a normal I_{Ca} trigger cannot activate SR Ca release when SR Ca load falls to ~50% of its normal value (11,12,31). It should be noted that this is similar to the $[Ca]_{SR}$ below which Ca sparks are not observed. We tested the possibility that the basis for this failure of ECC at low $[Ca]_{SR}$ is the same as in RyR gating properties, discussed above.

$[Ca]_{SR}$ was varied, and we simulated openings of one or two of the L-type Ca channels at each CaRU at different V_m. The unitary currents (in pA) were 0.666, 0.343, 0.147, and 0.053, at −20, 0, +20, and +40 mV, respectively. We estimate how many RyRs open when Ca enters via L-type Ca channels (Fig. 7). The rise of $[Ca]_{cleft}$ depends on V_m

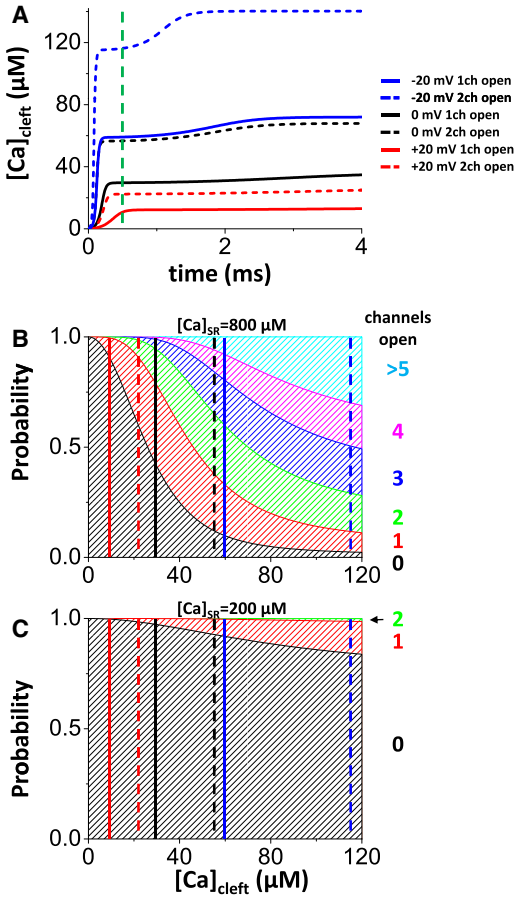

FIGURE 7 L-type I_{Ca} and induction of RyR channel opening. (*A*) Time course of $[Ca]_{cleft}$ during opening of one or two Ca channels at different V_m. (*B*) Probabilities that *n* RyR channels will open when the CaRU is exposed to $[Ca]_{Cleft}$ for 0.5 ms (open time) with high SR Ca load ($[Ca]_{SR}$ = 800 μM). (*C*) Same as *B* but for $[Ca]_{SR}$ = 200 μM.

and the number of open channels (Fig. 7 *A*). At V_m = −20 mV, a single L-type Ca channel opening can initiate a Ca spark at $[Ca]_{SR}$ = 800 μM (Fig. 7 *B*; compare with Fig. 3 *B*). That is, there is a high probability that two or more RyRs will be activated during the 0.5-ms open time expected (Fig. 7 *A*, *green line*). At more positive V_m, the unitary Ca current is smaller (lower driving force) and the possibility of Ca spark induction by a single L-type Ca channel opening is reduced. However, Ca-channel open probability is also higher at higher V_m, increasing the probability of multiple Ca-channel openings. Coincidentally, the efficacy of one open Ca channel at −20 mV is comparable to that of two channels at 0 mV (Fig. 7 *A*, *blue solid line* and *black dashed line*, respectively). On the other hand, if $[Ca]_{SR}$ is low (200 μM), even when the L-type current is large, the probability that Ca sparks will be initiated is zero (Fig. 7 *C*).

We also extended this to the full model and measured the gain of ECC and fractional SR Ca release (Fig. 8). At low $[Ca]_{SR}$, I_{Ca} fails to activate SR Ca release. As $[Ca]_{SR}$

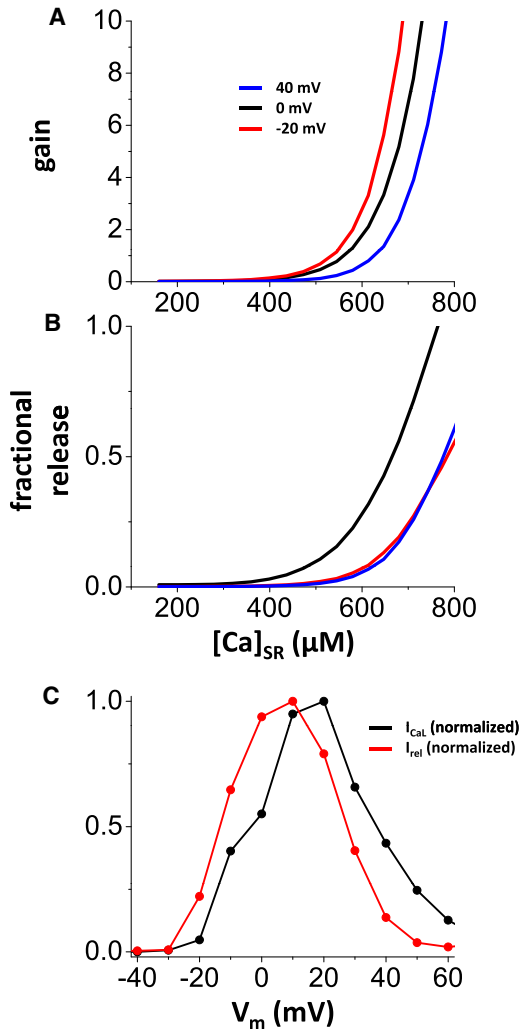

FIGURE 8 (*A*) ECC gain versus $[Ca]_{SR}$ at $V_m = -20$, 0, and +40 mV. Gain is defined by $\int I_{rel}/\int I_{CaL}$. (*B*) Fractional release versus $[Ca]_{SR}$ at $V_m = -20$, 0, and +40 mV. Fractional release is defined by $\int I_{rel}$/total SR Ca. (*C*) Normalized peak I_{Ca} and peak SR Ca release flux versus test V_m.

becomes higher, gain and fractional release both increase steeply. These results are similar to previous experimental findings (11,12,31). These curves also depend on the test V_m. If V_m is lower (−20 mV), unitary L-type Ca current becomes larger, and it is therefore more effective to initiate Ca sparks at lower $[Ca]_{SR}$. At higher V_m (+40 mV), although open probability is high and multiple L-type Ca channels open, the unitary L-type Ca current is small (0.053 pA), such that Ca sparks do not occur until a higher $[Ca]_{SR}$ is reached. This explains the higher ECC gain at negative V_m and causes the well-known displacement of the SR Ca-release curve to the left of the I_{Ca}-V_m dependence (Fig. 8 *C*)). In addition, fractional SR Ca release shows a similar shape, but is highest for 0 mV and almost the same for V_m= –20 and +40 mV. Fewer CaRUs fire at −20 mV, because the open probability of L-type Ca channels is relatively low (thus, some CaRUs will not have I_{Ca}), whereas at +40 mV, fewer junctions fire, because either the number of open channels is insufficient to make up for the lower unitary current (Fig. 7 *B*) or the openings are not adequately synchronous.

DISCUSSION

Increasing $[Ca]_{SR}$ enhances Ca sparks and waves

In this study, we analyze how stochastic opening of RyRs can initiate a Ca spark, and how $[Ca]_{SR}$ can profoundly influence the ability of a single RyR opening to initiate a Ca spark. The RyR channel is regulated by both $[Ca]_{Cleft}$ and $[Ca]_{SR}$. As $[Ca]_{SR}$ increases, RyRs are sensitized to open at lower $[Ca]_{Cleft}$ and for longer times (9,10,19). In this case, when one RyR opens, it is much more likely to recruit additional RyRs to open in the same CaRU, because $[Ca]_{SR}$ is high (which sensitizes the RyRs) and $[Ca]_{Cleft}$ is higher and lasts longer (enhancing the probability of stochastic RyR activation), and these effects work synergistically. Of course, initial RyR openings are also much more frequent at high $[Ca]_{SR}$ to begin with (for any $[Ca]_{Cleft}$). That further enhances the steep rise in Ca-spark frequency and SR Ca leak with increasing $[Ca]_{SR}$, as seen experimentally (5,10,32). Although not explicitly studied here, the higher propensity for Ca sparks as $[Ca]_{SR}$ increases would also greatly enhance the ability of individual Ca sparks to stimulate neighboring CaRU to also fire Ca sparks and propagate as Ca waves through myocytes. These Ca waves activate a depolarizing inward Na/Ca exchange current that can trigger inappropriate action potentials and triggered arrhythmias (33).

Reducing $[Ca]_{SR}$ prevents Ca sparks but not SR Ca leak

When $[Ca]_{SR}$ is reduced below a certain threshold level, Ca sparks effectively cease to occur. As Zima et al. (5) demonstrate, this is not because the Ca sparks are simply too small to measure at low $[Ca]_{SR}$. They showed that Ca sparks cease at $[Ca]_{SR}$ where the Ca-spark amplitude is far above the detection limit for Ca sparks. Our study provides clear mechanistically sound explanations for these observations, based on known properties of RyR gating.

Several factors (as discussed above) synergize to produce this apparently steep cessation of Ca sparks. First, the lower $[Ca]_{SR}$ reduces the driving force for Ca, resulting in lower $[Ca]_{Cleft}$ during an RyR opening, which is a weaker stimulus for neighboring RyRs. Second, RyR open time is lower at low $[Ca]_{SR}$, and this may also limit the rise in $[Ca]_{Cleft}$ and the likelihood of adjacent RyR activation. Third, the reduced open time at low $[Ca]_{SR}$ would reduce the time for stochastic activation of neighboring RyRs. Fourth, at low $[Ca]_{SR}$, the RyR is much less sensitive to activation by a given $[Ca]_{Cleft}$, and this effect synergizes with the other

three to greatly reduce the probability that a given RyR opening can initiate opening of multiple RyRs at a single CaRU. The lower $[Ca]_{SR}$ also reduces the probability that a first RyR opening will happen, and that effect will further reduce the probability for a Ca spark at low $[Ca]_{SR}$. To put this into a semiquantitative context, our analysis (Fig. 3 *A*) shows that a single RyR opening is ~1000 times less likely to trigger a second RyR for $[Ca]_{SR} = 200$ vs. 800 μM. If we multiply that by the 10- to 100-fold lower RyR P_o (Fig. 1 *C*, which reflects the reduced probability for a first event), that would make the overall probability of a Ca spark 10,000–100,000 times lower at 200 vs. 800 μM $[Ca]_{SR}$. This explains the apparently abrupt thresholdlike disappearance of Ca sparks as $[Ca]_{SR}$ declines in the data of Zima et al. (5).

It should be noted that SR Ca-release events smaller than Ca sparks have been reported, and these are referred to as Ca quarks or quarky Ca release (34,35). These may indeed reflect the same sub-spark-amplitude SR Ca-release events we (and Zima et al. (5)) are considering as nonspark RyR-mediated SR Ca leak. Here, we have focused on functionally homogeneous independent RyRs within CaRUs. However, it is also possible that individual RyRs or tiny clusters of RyRs that are not within the CaRU (or that have fundamentally different regulation) could contribute to nonspark-mediated SR Ca leak (4,36). Those rogue RyRs could certainly contribute to the nonspark-mediated SR Ca leak, and it is easy to appreciate how that could work, based on the principle examined here. If RyRs within a given CaRU are perforce functionally coupled such that when one opens they all open in a concerted fashion (37), then by definition one RyR opening must drive an entire CaRU, our analysis would be moot, and rogue RyRs would be required to explain RyR-mediated SR Ca leak that is smaller than such a unit. However, the real extent of coupled RyR gating in the heart is not known. If such coupling is weak and/or only involves 2–3 nearest neighbors, then our analysis remains qualitatively unaltered. Indeed, although rogue RyRs may well exist, our conclusion is that they are not necessary to explain SR Ca-release events that are smaller than a Ca spark. Indeed, other modeling studies have integrated SR Ca leak via Ca sparks and subspark events (25,38), including a contemporaneous study (39) where coupled RyR gating was relaxed to allow subspark leak to be significant, as seen in myocyte experiments (5,35).

It is important to acknowledge that our model, while reasonable in representing experimentally measured RyR properties, is unlikely to be completely accurate in all details. However, we are confident that any inaccuracies in our model will have only quantitative, not qualitative, impact on our conclusions. Moreover, the logical synergy of the known $[Ca]_{SR}$ effects explored here that produces the mechanistic conclusions above is compelling. We show data for CaRUs of only 100 RyRs, but the qualitative conclusions would be unaltered by a wide variety of CaRU sizes, or specific Ca dependences. Additional experimental work is likely to help refine the model and its parameters and sharpen the quantitative aspects of our conclusions.

Mean open time of RyRs

In our model, we varied RyR mean open time with $[Ca]_{SR}$ (between 0.7 and 1.9 ms) based on experimental observations by Gyöke et al. (19). Other groups observed less dependence of open time on $[Ca]_{SR}$. To test how important this is to our results, we also ran simulations where open time was independent of $[Ca]_{SR}$ ($k_{21} = k_{34}$=1.0 ms^{-1}). Fig. S5 shows that the leak curves are slightly shifted at $[Ca]_{SR}$ >550 μM, but that the fundamental characteristics are little changed. This indicates that $[Ca]_{SR}$-dependent alteration in open time is not essential for the observed behavior, and that the other factors we have explored are sufficient.

Reduced $[Ca]_{SR}$ reduces fractional SR Ca release during ECC

Some of the same characteristics that cause Ca spark failure at low $[Ca]_{SR}$ are also likely to explain the dramatic reduction in fractional SR Ca release seen at low $[Ca]_{SR}$ (11,12). Indeed, those studies showed that when diastolic SR Ca content falls by ~50%, normal L-type I_{Ca} can no longer trigger appreciably SR Ca release. There may be two explanations for this, but both are germane here. First, the normal I_{Ca}, which can activate SR Ca release with high fidelity at virtually all CaRUs when the SR is well loaded (40,41), may not produce high enough $[Ca]_{Cleft}$ to trigger RyR opening at low $[Ca]_{SR}$ because of the desensitization of RyR to $[Ca]_{Cleft}$ caused by low $[Ca]_{SR}$. This is similar to the effect in Fig. 1 *C*, where lower $[Ca]_{SR}$ reduces the P_o of RyR (by ~100-fold) over a broad range of $[Ca]_{Cleft}$. Second, even if local L-type Ca current activates a single RyR in a CaRU, the probability of a full activation at that CaRU when $[Ca]_{SR}$ is low (Fig. 8) is reduced for precisely the same reasons described above for the failure of Ca sparks after an initial RyR opening.

At more positive V_m, unitary i_{Ca} amplitude gets smaller, but more channels will open, the latency to opening is shorter, and thus, openings are more likely to overlap in time. This means that at high $[Ca]_{SR}$, either a single Ca channel opening (at −20 mV) or 2–3 relatively synchronized openings at V_m = 0–+20 mV can trigger SR Ca release at a CaRU with high coupling fidelity. It is apparent that the single opening at more negative potentials is a more efficient trigger, because ECC gain (release/trigger) is higher there (14,41). A consequence of that is that as a function of V_m, the Ca transient amplitude peaks at a slightly more negative V_m than the maximal I_{Ca} amplitude. The smaller Ca transients at lower V_m (Fig. 8 *B*) occur because fractional release becomes smaller (fewer sites are firing

(Fig. S7)), despite the higher i_{Ca} efficacy (or gain) at the CaRUs that do fire.

On the other hand, as $[Ca]_{SR}$ is reduced, all of these I_{Ca} triggers become less efficacious (Fig. 8), and that explains the failure of Ca-induced Ca-release at low $[Ca]_{SR}$. Flirting with the edge of this steep-gain phase can also cause instability evident as Ca and action potential alternans. Diaz et al. (42) demonstrated this phenomenon with V_m pulses to –20 mV. For their conditions, the I_{Ca} during the small beat was able to release Ca from only a modest fraction of CaRUs, resulting in a small overall Ca transient and less Ca-dependent inactivation of I_{Ca}. At the next beat, the SR Ca load was slightly higher, and the same I_{Ca} trigger caused more uniform and larger SR Ca release (presumably because the higher $[Ca]_{SR}$ allowed recruitment of more release sites). However, the larger Ca transient enhanced Ca extrusion and reduction of $[Ca]_{SR}$, causing the next Ca transient to be small and the alternating pattern to continue.

Basis for termination of SR Ca release during sparks and ECC

Several studies have shown that SR Ca release terminates during both ECC and Ca sparks when $[Ca]_{SR}$ falls to ~40–50% of the typical normal SR Ca content or $[Ca]_{SR}$ (11,12,33,41,43–49). That effect may also be related to this discussion and the importance of $[Ca]_{SR}$ in regulating SR Ca release. The current paradigm emerging from much work is as follows. Once regenerative SR Ca release has started at a CaRU, as either a Ca spark or a Ca spike or during normal ECC, $[Ca]_{SR}$ progressively declines, and at some point, the combination of $[Ca]_{SR}$-dependent desensitization of RyRs and lower $[Ca]_{Cleft}$ (as driving force and possibly open-time decline) causes SR Ca release to self-terminate at a threshold $[Ca]_{SR}$ (which is similar to the threshold for Ca sparks and for I_{Ca} to trigger SR Ca release). This is analogous to the relative inability of a single RyR opening to initiate a Ca spark at low $[Ca]_{SR}$, as discussed above.

Effect of HF and β-adrenergic stimulation

When RyR becomes more sensitive to $[Ca]_{Cleft}$, the Ca-spark flux rate shifts to lower $[Ca]_{SR}$ (Fig. S1 *A*). This happens during HF and β-adrenergic stimulation. Although RyR becomes sensitive during HF, the SERCA pump is also down-regulated. Therefore, $[Ca]_{SR}$ falls, and Ca sparks are rare. However, in this state, adrenergic activation (ISO) can drive $[Ca]_{SR}$ up to the point where Ca sparks are more likely.

CONCLUSION

In this study, we show how RyR channel properties are linked to Ca sparks and nonspark Ca leak. Several factors contribute synergistically to the failure of Ca-spark initiation as $[Ca]_{SR}$ declines: 1), the lower $[Ca]_{SR}$ reduces the RyR Ca driving force and thus limits kinetics and amplitude of local $[Ca]_{Cleft}$ rise; 2), low $[Ca]_{SR}$ can reduce RyR open time (τ_O), which further limits the local $[Ca]_{Cleft}$ attained; 3), the low τ_O and fast $[Ca]_{Cleft}$ dissipation after closure shorten the opportunity for neighboring RyR activation; and 4), at low $[Ca]_{SR}$, the RyR exhibits reduced $[Ca]_{Cleft}$ sensitivity. We conclude that all of these factors synergize to reduce the probability of Ca sparks as $[Ca]_{SR}$ declines, despite continued RyR-mediated SR Ca leak. We further suggest that these effects are directly and mechanistically related to the control of both initiation and termination of Ca sparks, to arrhythmogenic Ca-wave propagation initiating delayed afterdepolarizations, and to the control of fractional SR Ca release during ECC.

SUPPORTING MATERIAL

Details of the subcellular Ca cycling model, a detailed discussion of equations and parameters, references, seven figures, and three tables are available at http://www.biophysj.org/biophysj/supplemental/S0006-3495(11)01207-0.

This work was supported by a postdoctoral fellowship from the American Heart Association, Western States Affiliate (D.S.), and by National Institutes of Health grant R37-HL30077 (D.M.B.).

REFERENCES

1. Bers, D. M. 2001. Excitation Contraction Coupling and Cardiac Contractile Force. Kluwer Academic, Boston.
2. George, C. H. 2008. Sarcoplasmic reticulum Ca^{2+} leak in heart failure: mere observation or functional relevance? *Cardiovasc. Res.* 77: 302–314.
3. Chelu, M. G., and X. H. Wehrens. 2007. Sarcoplasmic reticulum calcium leak and cardiac arrhythmias. *Biochem. Soc. Trans.* 35: 952–956.
4. Santiago, D. J., J. W. Curran, …, T. R. Shannon. 2010. Ca sparks do not explain all ryanodine receptor-mediated SR Ca leak in mouse ventricular myocytes. *Biophys. J.* 98:2111–2120.
5. Zima, A. V., E. Bovo, …, L. A. Blatter. 2010. Ca^{2+} spark-dependent and -independent sarcoplasmic reticulum Ca^{2+} leak in normal and failing rabbit ventricular myocytes. *J. Physiol.* 588:4743–4757.
6. Franzini-Armstrong, C., F. Protasi, and V. Ramesh. 1999. Shape, size, and distribution of Ca^{2+} release units and couplons in skeletal and cardiac muscles. *Biophys. J.* 77:1528–1539.
7. Soeller, C., D. Crossman, …, M. B. Cannell. 2007. Analysis of ryanodine receptor clusters in rat and human cardiac myocytes. *Proc. Natl. Acad. Sci. USA.* 104:14958–14963.
8. Soeller, C., I. D. Jayasinghe, …, M. B. Cannell. 2009. Three-dimensional high-resolution imaging of cardiac proteins to construct models of intracellular Ca^{2+} signalling in rat ventricular myocytes. *Exp. Physiol.* 94:496–508.
9. Lukyanenko, V., I. Györke, and S. Györke. 1996. Regulation of calcium release by calcium inside the sarcoplasmic reticulum in ventricular myocytes. *Pflugers Arch.* 432:1047–1054.
10. Shannon, T. R., K. S. Ginsburg, and D. M. Bers. 2002. Quantitative assessment of the SR Ca^{2+} leak-load relationship. *Circ. Res.* 91: 594–600.

11. Bassani, J. W., W. Yuan, and D. M. Bers. 1995. Fractional SR Ca release is regulated by trigger Ca and SR Ca content in cardiac myocytes. *Am. J. Physiol.* 268:C1313–C1319.
12. Shannon, T. R., K. S. Ginsburg, and D. M. Bers. 2000. Potentiation of fractional sarcoplasmic reticulum calcium release by total and free intra-sarcoplasmic reticulum calcium concentration. *Biophys. J.* 78:334–343.
13. Fabiato, A., and F. Fabiato. 1979. Use of chlorotetracycline fluorescence to demonstrate Ca^{2+}-induced release of Ca^{2+} from the sarcoplasmic reticulum of skinned cardiac cells. *Nature.* 281:146–148.
14. Cannell, M. B., J. R. Berlin, and W. J. Lederer. 1987. Effect of membrane potential changes on the calcium transient in single rat cardiac muscle cells. *Science.* 238:1419–1423.
15. Lukyanenko, V., I. Györke, …, S. Györke. 2000. Inhibition of $Ca(^{2+})$ sparks by ruthenium red in permeabilized rat ventricular myocytes. *Biophys. J.* 79:1273–1284.
16. Kettlun, C., A. González, …, M. Fill. 2003. Unitary Ca^{2+} current through mammalian cardiac and amphibian skeletal muscle ryanodine receptor channels under near-physiological ionic conditions. *J. Gen. Physiol.* 122:407–417.
17. Mejía-Alvarez, R., C. Kettlun, …, M. Fill. 1999. Unitary Ca^{2+} current through cardiac ryanodine receptor channels under quasi-physiological ionic conditions. *J. Gen. Physiol.* 113:177–186.
18. Cannell, M. B., and C. Soeller. 1997. Numerical analysis of ryanodine receptor activation by L-type channel activity in the cardiac muscle diad. *Biophys. J.* 73:112–122.
19. Györke, I., and S. Györke. 1998. Regulation of the cardiac ryanodine receptor channel by luminal Ca^{2+} involves luminal Ca^{2+} sensing sites. *Biophys. J.* 75:2801–2810.
20. Stern, M. D., and E. G. Lakatta. 1992. Excitation-contraction coupling in the heart: the state of the question. *FASEB J.* 6:3092–3100.
21. Stern, M. D. 1992. Theory of excitation-contraction coupling in cardiac muscle. *Biophys. J.* 63:497–517.
22. Restrepo, J. G., J. N. Weiss, and A. Karma. 2008. Calsequestrin-mediated mechanism for cellular calcium transient alternans. *Biophys. J.* 95:3767–3789.
23. Shannon, T. R., F. Wang, …, D. M. Bers. 2004. A mathematical treatment of integrated Ca dynamics within the ventricular myocyte. *Biophys. J.* 87:3351–3371.
24. Picht, E., A. V. Zima, …, D. M. Bers. 2007. SparkMaster: automated calcium spark analysis with ImageJ. *Am. J. Physiol. Cell Physiol.* 293:C1073–C1081.
25. Hartman, J. M., E. A. Sobie, and G. D. Smith. 2010. Spontaneous Ca^{2+} sparks and Ca^{2+} homeostasis in a minimal model of permeabilized ventricular myocytes. *Am. J. Physiol. Heart Circ. Physiol.* 299: H1996–H2008.
26. Shannon, T. R., F. Wang, and D. M. Bers. 2005. Regulation of cardiac sarcoplasmic reticulum Ca release by luminal [Ca] and altered gating assessed with a mathematical model. *Biophys. J.* 89:4096–4110.
27. Shannon, T. R., S. M. Pogwizd, and D. M. Bers. 2003. Elevated sarcoplasmic reticulum Ca^{2+} leak in intact ventricular myocytes from rabbits in heart failure. *Circ. Res.* 93:592–594.
28. Li, Y., E. G. Kranias, …, D. M. Bers. 2002. Protein kinase A phosphorylation of the ryanodine receptor does not affect calcium sparks in mouse ventricular myocytes. *Circ. Res.* 90:309–316.
29. Curran, J., M. J. Hinton, …, T. R. Shannon. 2007. β-adrenergic enhancement of sarcoplasmic reticulum calcium leak in cardiac myocytes is mediated by calcium/calmodulin-dependent protein kinase. *Circ. Res.* 100:391–398.
30. Curran, J., K. H. Brown, …, T. R. Shannon. 2010. Spontaneous Ca waves in ventricular myocytes from failing hearts depend on Ca^{2+}-calmodulin-dependent protein kinase II. *J. Mol. Cell. Cardiol.* 49:25–32.
31. Trafford, A. W., M. E. Díaz, …, D. A. Eisner. 1997. Enhanced Ca^{2+} current and decreased Ca^{2+} efflux restore sarcoplasmic reticulum Ca^{2+} content after depletion. *Circ. Res.* 81:477–484.
32. Györke, S., I. Györke, …, T. F. Wiesner. 2002. Regulation of sarcoplasmic reticulum calcium release by luminal calcium in cardiac muscle. *Front. Biosci.* 7:d1454–d1463.
33. Pogwizd, S. M., and D. M. Bers. 2002. Calcium cycling in heart failure: the arrhythmia connection. *J. Cardiovasc. Electrophysiol.* 13:88–91.
34. Lipp, P., and E. Niggli. 1996. Submicroscopic calcium signals as fundamental events of excitation—contraction coupling in guinea-pig cardiac myocytes. *J. Physiol.* 492:31–38.
35. Brochet, D. X. P., W. Xie, …, W. J. Lederer. 2011. Quarky calcium release in the heart. *Circ. Res.* 108:210–218.
36. Sobie, E. A., S. Guatimosim, …, W. J. Lederer. 2006. The Ca $^{2+}$ leak paradox and rogue ryanodine receptors: SR Ca $^{2+}$ efflux theory and practice. *Prog. Biophys. Mol. Biol.* 90:172–185.
37. Marx, S. O., J. Gaburjakova, …, A. R. Marks. 2001. Coupled gating between cardiac calcium release channels (ryanodine receptors). *Circ. Res.* 88:1151–1158.
38. Hashambhoy, Y. L., J. L. Greenstein, and R. L. Winslow. 2010. Role of CaMKII in RyR leak, EC coupling and action potential duration: a computational model. *J. Mol. Cell. Cardiol.* 49:617–624.
39. Williams, G. S., A. C. Chikando, …, M. S. Jafri. 2011. Dynamics of calcium sparks and calcium leak in the heart. *Biophys. J.* 101:1287–1296.
40. Inoue, M., and J. H. B. Bridge. 2003. Ca^{2+} sparks in rabbit ventricular myocytes evoked by action potentials: involvement of clusters of L-type Ca^{2+} channels. *Circ. Res.* 92:532–538.
41. Altamirano, J., and D. M. Bers. 2007. Voltage dependence of cardiac excitation-contraction coupling: unitary Ca^{2+} current amplitude and open channel probability. *Circ. Res.* 101:590–597.
42. Díaz, M. E., S. C. O'Neill, and D. A. Eisner. 2004. Sarcoplasmic reticulum calcium content fluctuation is the key to cardiac alternans. *Circ. Res.* 94:650–656.
43. Trafford, A. W., M. E. Díaz, …, D. A. Eisner. 2000. Modulation of CICR has no maintained effect on systolic Ca^{2+}: simultaneous measurements of sarcoplasmic reticulum and sarcolemmal Ca^{2+} fluxes in rat ventricular myocytes. *J. Physiol.* 522:259–270.
44. Shannon, T. R., T. Guo, and D. M. Bers. 2003. Ca^{2+} scraps: local depletions of free $[Ca^{2+}]$ in cardiac sarcoplasmic reticulum during contractions leave substantial Ca^{2+} reserve. *Circ. Res.* 93:40–45.
45. Guo, T., X. Ai, …, D. M. Bers. 2007. Intra-sarcoplasmic reticulum free $[Ca^{2+}]$ and buffering in arrhythmogenic failing rabbit heart. *Circ. Res.* 101:802–810.
46. Zima, A. V., E. Picht, …, L. A. Blatter. 2008. Termination of cardiac Ca^{2+} sparks: role of intra-SR $[Ca^{2+}]$, release flux, and intra-SR Ca^{2+} diffusion. *Circ. Res.* 103:e105–e115.
47. Picht, E., A. V. Zima, …, D. M. Bers. 2011. Dynamic calcium movement inside cardiac sarcoplasmic reticulum during release. *Circ. Res.* 108:847–856.
48. Sobie, E. A., K. W. Dilly, …, M. S. Jafri. 2002. Termination of cardiac Ca^{2+} sparks: an investigative mathematical model of calcium-induced calcium release. *Biophys. J.* 83:59–78.
49. Terentyev, D., S. Viatchenko-Karpinski, …, S. Györke. 2002. Luminal Ca^{2+} controls termination and refractory behavior of Ca^{2+}-induced Ca2+ release in cardiac myocytes. *Circ. Res.* 91:414–420.